Eur. Phys. J. Spec. Top. (2025) 234:3007–3013
https://doi.org/10.1140/epjs/s11734-025-01599-8

THE EUROPEAN PHYSICAL JOURNAL SPECIAL TOPICS

Regular Article

Morphology studies on craters created by femtosecond laser irradiation in UDMA polymer targets embedded with plasmonic gold nanorods

Ágnes Nagyné Szokol[1,2,a], Judit Kámán[1], Roman Holomb[1], István Rigó[1], Márk Aladi[1], Miklós Kedves[1], Béla Ráczkevi[1], Péter Rácz[1], Attila Bonyár[3], Alexandra Borók[3], Shereen Zangana[3], Melinda Szalóki[4], István Papp[1], Gábor Galbács[5], Tamás S. Biró[1,6,7], László P. Csernai[1,8,9], Norbert Kroó[1,10], Miklós Veres[1], and NAPLIFE Collaboration

[1] HUN-REN Wigner Research Centre for Physics, Budapest 1121, Hungary
[2] University of Pécs, Pecs, Hungary
[3] Department of Electronics Technology, Faculty of Electrical Engineering and Informatics, Budapest University of Technology and Economics, Budapest 1111, Hungary
[4] Department of Biomaterials and Prosthetic Dentistry, Faculty of Dentistry, University of Debrecen, Debrecen 4032, Hungary
[5] Department of Inorganic and Analytical Chemistry, University of Szeged, Szeged 6720, Hungary
[6] Institute for Physics, Babeş Bolyai University, 3400 Cluj-Napoca, Romania
[7] Complexity Science Hub, 1080 Vienna, Austria
[8] Department of Physics and Technology, Bergen University, 5020 Bergen, Norway
[9] Csernai Consult, 5119 Bergen, Norway
[10] Hungarian Academy of Sciences, Budapest 1051, Hungary

Received 19 December 2024 / Accepted 13 March 2025 / Published online 3 April 2025

Abstract The effect of embedded plasmonic gold nanoparticles on the crater morphology was studied in 160 µm-thick UDMA–TEGDMA copolymer films irradiated by femtosecond single pulses of a Ti:Sa laser. The plasmonic absorption of the embedded gold nanorods had a resonance at the wavelength of the laser. It was observed that by increasing the laser intensity the diameter of the craters decreased, while the depth of the craters increased. In addition, the crater depths were significantly higher in the presence of gold nanorods. A threshold intensity of $1.5 \cdot 10^{17}$ W/cm^2 has been determined, above which a doubled roughness and sevenfold increased crater volume was observed in the polymer containing gold nanorods.

Graphical abstract

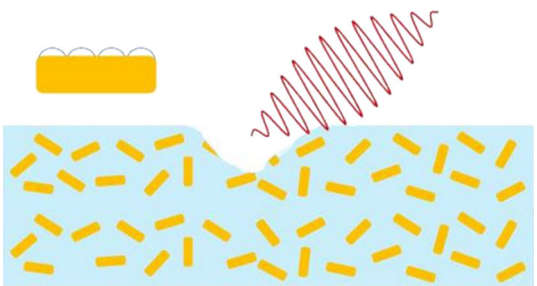

[a] e-mail: szokol.agnes@wigner.hun-ren.hu (corresponding author)

1 Introduction

The behaviour of polymers under laser irradiation is extensively studied and has wide literature as this treatment allows to control their optical, thermophysical, electrical and other properties. The application of this technique is extensive starting with directed creation of surface structures [1, 2], through ultrafast laser micro-machining [3] to aeronautic applications [4]. Polymers can be used not just as a device or tool but as a matrix and fuel at the same time [5].

Among the published research, only a few are devoted to the interaction of high-intensity laser pulses with polymers containing plasmonic gold nanoparticles. Through the collective oscillation of their free electrons coupled resonantly to the electromagnetic field of light in their vicinity these nanostructures could enhance various laser-matter interactions, like Raman scattering [6], fluorescence [7] or absorption [8]. With plasmonics a 3–4 orders of magnitude amplification of the electric field can be achieved [9], which can create ultra-high laser fields in the surrounding of the nanoparticles [10]. Under these conditions protons can be accelerated to the level being sufficient to initiate nuclear fusion [11].

The enhanced absorption due to plasmonic nanoparticles should also be reflected in the macroscopic outcomes of laser-matter interaction. For example, there should be differences in the ablation and crater formation during the irradiation of a material with and without embedded plasmonic gold nanorods by a high-intensity femtosecond laser pulse. The aim of this work was to study the effect of plasmonic gold nanorods on the morphology and dimensions of craters formed in a polymer upon irradiation with single-shot laser pulses of different intensity. White light interferometry was used to record the 3D surface morphology and to determine the main geometric properties (such as depth, roughness and volume) of the craters formed by femtosecond laser pulses of different intensity.

2 Materials and methods

The two samples were prepared as it was presented in Ref. [12]. Both are based on a photopolymer matrix, one with gold nanorods (marked as Au2) and one without them (Au0, handled as a reference). The parameters of the gold nanorods were chosen so that their plasmonic absorption is resonant to the wavelength of the femtosecond laser (795 nm) used later for irradiation [11, 13, 14]. Urethane dimethacrylate and triethylene glycol dimethacrylate was mixed in 3:1 weight ratio to get the polymer matrix. The plasmonic nanoparticles capped with dodecanethiol were added to the mixture and stirred by ultrasound bathing to get a homogeneous mixture. The photopolymerization was performed between two glass plate by a normal dental cure lamp.

The laser irradiation experiments on the polymer targets were performed in a vacuum chamber evacuated to 10^{-6} Pa pressure with a Coherent Hidra laser system having 795 nm central wavelength and 42 fs pulse length. The focused beam of the laser provides intensities on the order of 10^{16}–10^{17} W/cm^2. The irradiations were implemented with two different pulse energies: 10 mJ and 25 mJ (Au2 sample)/27 mJ (Au0 sample). The incident beam reached the surface of the target under 45°. Each treatment consisted of a single laser pulse. The intensity of the pulse was changed by moving the sample in 0.2 mm steps along the laser beam by a motorized stage. The sample was moved laterally after every shot, so the next laser pulse reached an untouched surface.

Morphology measurements were carried out by a white light interferometer (Zygo NewView 7100, HUN-REN Wigner RCP, Budapest, Hungary) which ensured non-contact and non-destructive circumstances to investigate the surface of the craters created during the irradiation of the polymer with single laser shots. The instrument can achieve 0.1 nm vertical and 0.52 μm lateral resolution. The measurements were performed with a 50 × Mirau objective having 0.19 mm × 0.14 mm field of view. Stitching was used to cover the whole crater area. The dimensions and other properties of the recorded surfaces were determined by using the built-in functions of the Zygo instrument software [15].

3 Results and discussion

3.1 Crater morphology

The crater surface changed as the polymer target surface was moved through the focal plane of the laser. Figure 1 compares the changes in the crater morphology in targets with and without plasmonic gold nanorods at low energy (10 mJ) and higher energy (27.7 or 25 mJ) irradiations. The middle column shows craters created with the polymer surface being at the focal spot; thus, those got the laser pulse with highest intensity. The two other columns show the craters created in out-of-focus conditions. We can observe that the in-focus craters are much smaller than those

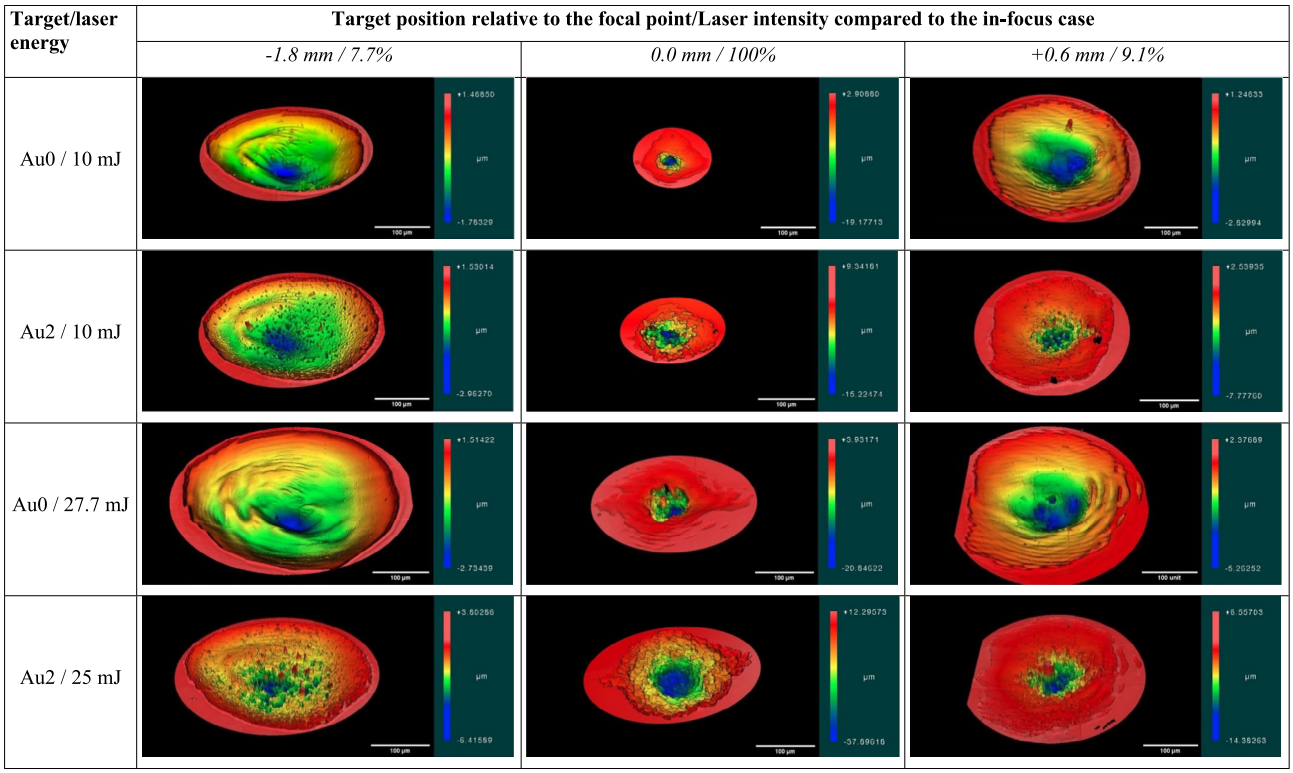

Fig. 1 White light interferometry images of the craters formed during the irradiation with low (top two) and high-energy (bottom two) laser pulse of polymer without (Au0) and with (Au2) plasmonic gold nanorods. The three columns represent the longitudinally after out-of-focus (left), in-focus (center) and before out-of-focus (right) conditions

formed with out-of-focus laser shots. It is evident that structure of each crater surface produced in the sample containing gold nanoparticles differs from those which were created in the polymer without gold.

3.2 Crater parameters

Figure 2 shows the deepest profiles of each crater formed in different longitudinal out-of-focus and in-focus positions of the target surface relative to the laser focal point. It can be seen that the crater size strikingly changes as a function of the distance from the focal point when the samples are irradiated with 10 mJ laser pulse energy (top left in Fig. 2). The deepest crater, with approx. 21 µm depth is formed in the in-focus case, and the depth decreases to 2 µm as the sample is moved away in both directions. The opposite can be observed for the crater diameter: as expected, it increases as the sample becomes out-of-focus, where the laser spot is larger.

The same behaviour can be observed for the sample containing gold nanoparticles, with similar crater sizes for 10 mJ irradiation energy (top right in Fig. 2). The largest crater depth is approx. 28 µm, and the smallest is around 2 µm. A comparison of the crater profiles for the two samples clearly shows the difference in their morphology described earlier, with smooth crater walls for the undoped target and rippled for the gold-containing one.

The formation of larger craters at higher pulse energies is reflected in their crater profiles as well, together with the differences between the wall morphologies for the doped and undoped cases. For the undoped sample, the largest crater depth for the 27.5 mJ irradiation is 33 µm, while for the Au-containing target irradiated with 25 mJ energy it is much larger, around 45 µm. As in the low-energy case, moving the target out of the focus results in shallower, but wider craters.

The change of the crater depth with the laser intensity at the target surface is shown in Fig. 3. It can be seen that at the low-energy irradiations the Au2 depths are slightly under the values measured in the Au0 craters at lower intensities, but they increase overall. Above 4.5×10^{16} W/cm^2 the depths continue to grow in both samples, but at craters in sample Au2 the maximal depth starts to be more prominent. For high laser pulse energy, however, the presence of the plasmonic nanoparticles results in deeper craters, being cca. 1.5-times as deep for the highest laser intensities, as those formed in the undoped target during the irradiation with slightly higher energy.

As the analysis of the crater morphologies revealed, the walls of formed craters are different for the undoped and doped targets: while they are smooth for the former, a rippled surface is formed in the case of the latter. In order to quantify this difference, the quadratic (Sq) and averaged (Sa) surface roughness values were calculated from

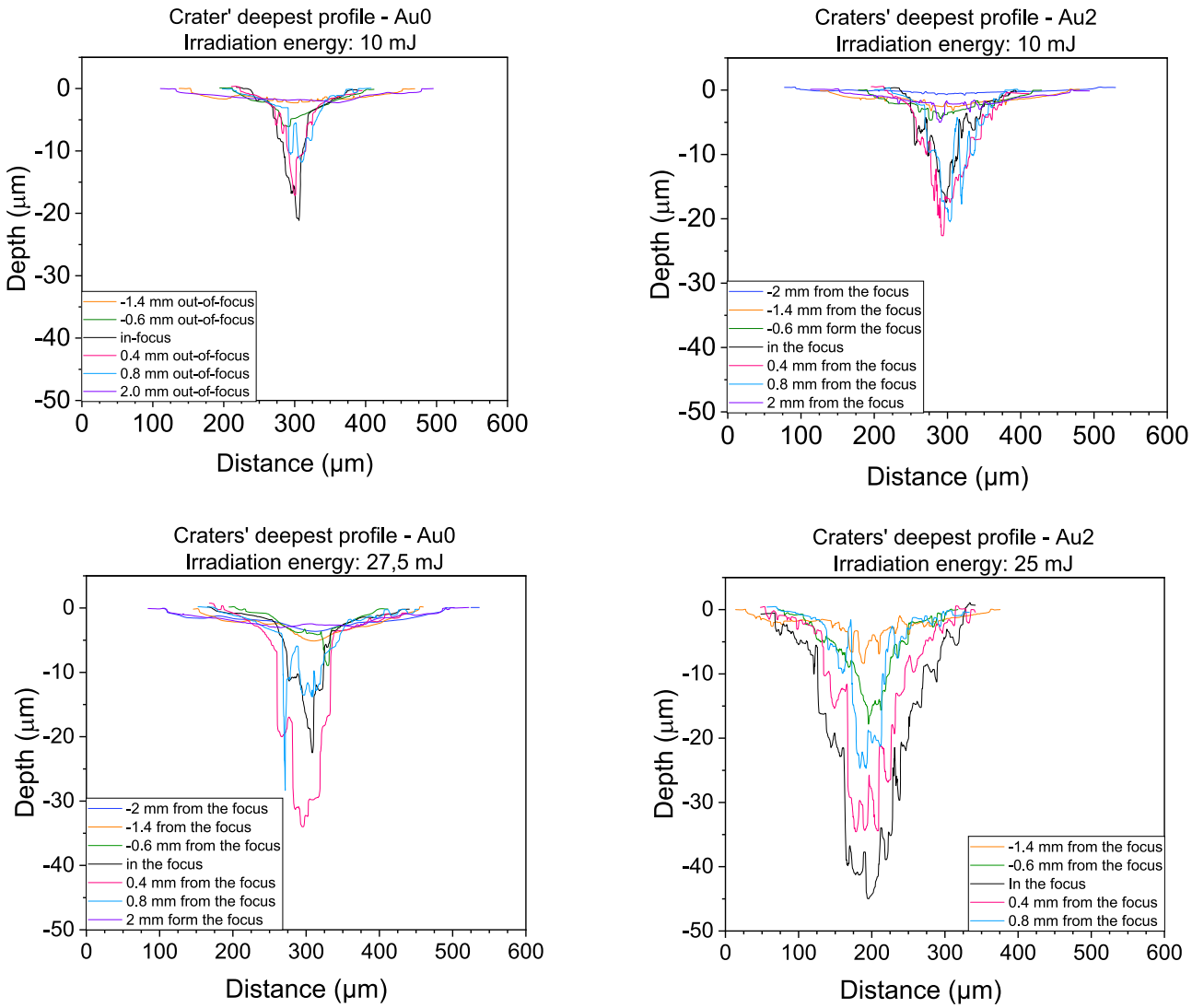

Fig. 2 The deepest profile of craters created at different focal distances. The irradiation was carried out with single laser shots of low (10 mJ, top row) and high (27.5 mJ and 25 mJ, bottom row) pulse energies for the samples without gold nanoparticles (Au0, left) and with embedded gold nanorods (Au2, right)

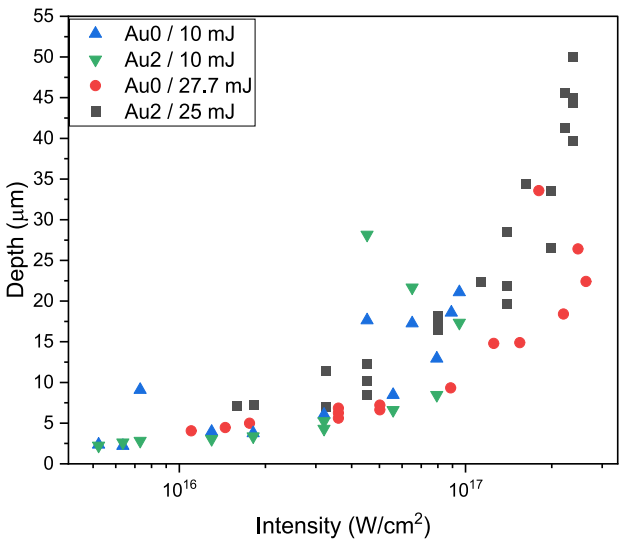

Fig. 3 Change of the crater depth with the laser intensity for low- and high-energy laser irradiations of the undoped (Au0) and gold nanorod-containing (Au2) targets

the white light interferometric images. The results for the high-energy irradiated undoped and doped samples are shown in Fig. 4. The figure shows that the increase in the laser intensity causes a rise in the surface roughness. For the undoped sample, the Sa values range between 0.67 and 1.37 μm (for 1.11×10^{16} and 1.25×10^{17} W/cm^2 laser intensities, respectively), while for the gold-doped one—between 0.73 and 9.27 μm (for 1.59×10^{16} and 1.13×10^{17} W/cm^2, respectively). While the values for the lowest laser intensity are similar, there is a remarkable, almost sevenfold difference for the highest intensity case. These findings support the conclusions made from the surface morphologies.

The effect of the gold nanoparticles is more striking when looking at the volumes of the formed craters (Fig. 5). In accordance with the previous findings, there is no significant difference between the two target types for the 10 mJ irradiations, where the highest laser intensity is around 10^{17} W/cm^2. The crater volume decreases with the laser intensity, from 0.85×10^5 μm^3 (5.2×10^{15} W/cm^2 laser intensity) to 0.20×10^5 μm^3 (9.5×10^{16} W/cm^2 laser intensity). A similar tendency can be observed in the crater volumes for the high-energy irradiation case up to around 1.5×10^{17} W/cm^2 laser intensity. In this region the crater volumes for the undoped and doped samples are also similar and slowly decrease from 1.28×10^5 μm^3 (1.1×10^{16} W/cm^2 laser intensity) to 0.44×10^5 μm^3 (8.8×10^{16} W/cm^2 laser intensity). Obviously, the volumes are higher than for the 10 mJ irradiations.

A different behaviour can be observed in the dependence of the crater volume on the intensity above the 1.5×10^{17} W/cm^2 threshold. While the volume shows some slight increase with the intensity for the undoped sample, it rapidly rises for the Au2 sample. A 1.7-times increase in the intensity results a 6.8-fold larger crater volume.

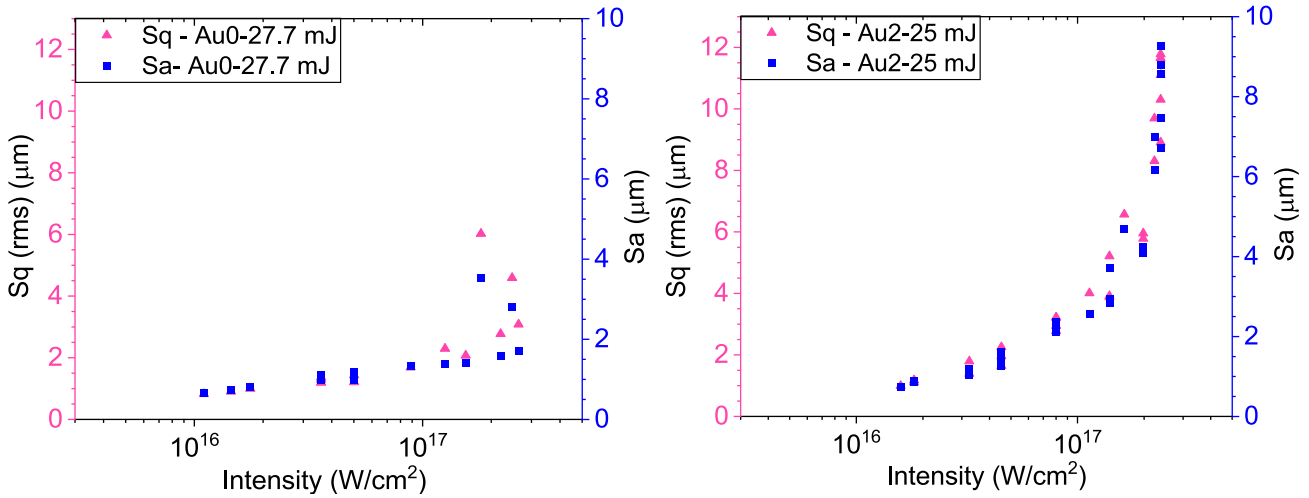

Fig. 4 Quadratic mean (Sq, left axis) and average surface roughness (Sa, right axis) values of the craters formed during the high-energy irradiation of the undoped (left) and doped (right) polymer targets with different laser intensities

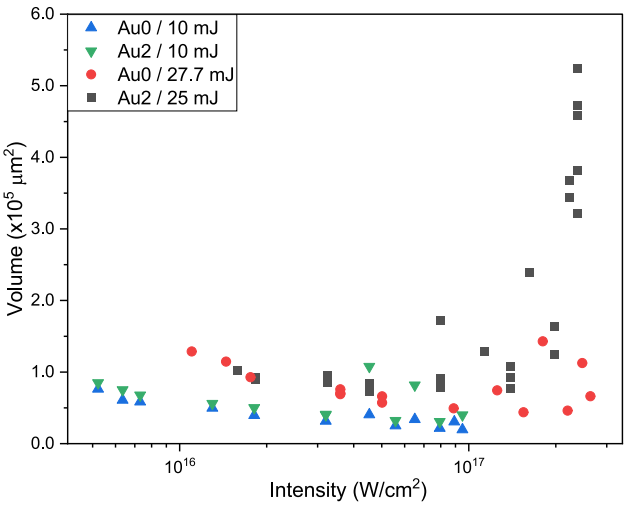

Fig. 5 Change of the crater volume with the laser intensity for low- and high-energy laser irradiations of the undoped and gold nanorod-containing targets

4 Conclusions

The crater formation was studied during the single-shot irradiation of undoped and doped with plasmonic gold nanoparticles polymer targets with focused femtosecond laser pulses. Two series of experiments were performed on the two types of samples with 10 mJ and 25.0/27.7 mJ pulse energies and with different laser intensities, adjust by changing the longitudinal position of the target surface relative to the focal plane. While similar craters are forming in both undoped and doped targets below 1.5×10^{17} W/cm^2 laser intensity, the presence of the nanoparticles leads to the formation of larger craters above this threshold. Here the crater volume increases with laser intensity, especially in the gold-doped target, where the 1.7-fold increase of the laser intensity is accompanied by an almost sevenfold larger crater volume.

Acknowledgements This work is supported in part by the Hungarian Research Network, Laser Fusion Research Laboratory under project Nr-s NKFIH-874-2/2020, NKFIH-468-3/2021, 2022-2.1.1-NL-2022-00002. The work was carried out in the HUN-REN Wigner Research Centre for Physics. We thank all the researchers inside the NAPLIFE project for their respective contributions to the success of this program: M. Csete, D. Vass, A. Szenes, E. Tóth, D. Palásti, Á. Bélteki at the Szeged University, A. Kumari, N. Abdulameer, A. Kumari, Á. Inger, K. Zhukovsky.

Author contributions

Á.N.Sz., J.K., R.H., and I.R.: measurements; Á.N.Sz., V.M., K.N., J.K., and T.S.B.: evaluation of measurements; Á.N.Sz.: prepared figures; M.A., M.K., B.R., and P.R.: laser irradiation; A.B., A.B., S.Z., and M.Sz.: sample preparation; I.P., L.CS., and N.K.: theory; Á.N.Sz., M.V., N.K., G.G., and T.S.B.: preparation of the manuscript.

Funding Open access funding provided by HUN-REN Wigner Research Centre for Physics.

Data availability statement Contact Ágnes Nagyné Szokol, szokol.agnes@wigner.hun-ren.hu, for further details on the data. No data associated in the manuscript.

Declarations

Conflict of interest The authors have no competing interests to declare that are relevant to the content of this article.

References

1. E. Rebollar, M. Castillejo, T.A. Ezquerra, Laser induced periodic surface structures on polymer films: from fundamentals to applications. Eur. Polym. J. **73**, 162–174 (2015). https://doi.org/10.1016/j.eurpolymj.2015.10.012
2. J. Hrabovský, C. Liberatore, I. Mirza, J. Sládek, J.T. Beranek, A.V. Bulgakov, N.M. Bulgakova, Surface structuring of Kapton polyimide with femtosecond and picosecond IR laser pulses. Interfacial Phenom. Heat Transf. **7**(2), 113–121 (2019). https://doi.org/10.1615/InterfacPhenomHeatTransfer.2019031067
3. I. Antanavičiūtė, L. Šimatonis, O. Ulčinas, A. Gadeikytė, B. Abakevičienė, S. Tamulevičius, V. Mikalayeva, V.A. Skeberdis, E. Stankevičius, T. Tamulevičius, Femtosecond laser micro-machined polyimide films for cell scaffold applications. J. Tissue Eng. Regen. Med. **12**(2), e760–e773 (2018). https://doi.org/10.1002/term.2376
4. M. Lu, M. Zhang, K. Zhang, Q. Meng, X. Zhang, Femtosecond UV laser ablation characteristics of polymers used as the matrix of astronautic composite material. Materials (Basel) **15**(19), 6771 (2022). https://doi.org/10.3390/ma15196771
5. N. Kroó, M. Aladi, M. Kedves, B. Ráczkevi, A. Kumari, P. Rácz, M. Veres, G. Galbács, L.P. Csernai, T.S. Biró, Monitoring of nanoplasmonics-assisted deuterium production in a polymer seeded with resonant Au nanorods using in situ femtosecond laser induced breakdown spectroscopy. Sci. Rep. **14**, 18288 (2024). https://doi.org/10.1038/s41598-024-69289-4
6. L. Mikac, I. Rigó, M. Škrabić, M. Ivanda, M. Veres, Comparison of glyphosate detection by surface-enhanced Raman spectroscopy using gold and silver nanoparticles at different laser excitations. Molecules **27**(18), 5767 (2022). https://doi.org/10.3390/molecules27185767

7. A. Sultangaziyev, R. Bukasov, Review: applications of surface-enhanced fluorescence (SEF) spectroscopy in bio-detection and biosensing. Sens. Bio-Sens. Res. **30**, 100382 (2020). https://doi.org/10.1016/j.sbsr.2020.100382
8. J. Kozuch, K. Ataka, J. Heberle, Surface-enhanced infrared absorption spectroscopy. Nat. Rev. Methods Prim. **3**, 70 (2023). https://doi.org/10.1038/s43586-023-00253-8
9. P.L. Stiles, J.A. Dieringer, N.C. Shah, R.P. Van Duyne, Surface-enhanced Raman spectroscopy. Annu. Rev. Anal. Chem. **1**(1), 601–626 (2008)
10. M.P. Mcoyi, K.T. Mpofu, M. Sekhwama, P. Mthunzi-Kufa, Developments in localized surface plasmon resonance. Plasmonics (2024). https://doi.org/10.1007/s11468-024-02620-x
11. I. Papp, L. Bravina, M. Csete, A. Kumari, I.N. Mishustin, A. Motornenko, P. Rácz, L.M. Satarov, H. Stöcker, D.D. Strottman, A. Szenes, D. Vass, Á.N. Szokol, J. Kámán, A. Bonyár, T.S. Biró, L.P. Csernai, N. Kroó, Kinetic model of resonant nanoantennas in polymer for laser induced fusion. Front. Phys. (2023). https://doi.org/10.3389/fphy.2023.1116023
12. A. Bonyár, M. Szalóki, A. Borók, I. Rigó, J. Kámán, S. Zangana, M. Veres, P. Rácz, M. Aladi, M. Kedves, Á. Szokol, P. Petrik, Z. Fogarassy, K. Molnár, M. Csete, A. Szenes, E. Tóth, D. Vas, I. Papp, G. Galbács, L.P. Csernai, T.S. Bíró, N. Kroó, NAPLIFE Collaboration, The effect of femtosecond laser irradiation and plasmon field on the degree of conversion of a UDMA–TEGDMA copolymer nanocomposite doped with gold nanorods. Int. J. Mol. Sci. **23**, 21. Paper: 13575 (2022). https://doi.org/10.3390/ijms232113575
13. M. Csete, A. Szenes, E. Tóth, D. Vass, O. Fekete, B. Bánhelyi, I. Papp, T. Bíró, L.P. Csernai, N. Kroó, Comparative study on the uniform energy deposition achievable via optimized plasmonic nanoresonator distributions. Plasmonics **17**, 775–787 (2022). https://doi.org/10.1007/s11468-021-01571-x
14. L.P. Csernai, M. Csete, I.N. Mishustin, A. Motornenko, I. Papp, L.M. Satarov, H. Stöcker, N. Kroo, NAPLIFE Collaboration, Radiation dominated implosion with flat target. Phys. Wave Phenom. **28**(3), 187–199 (2020). https://doi.org/10.3103/S1541308X20030048. arXiv:1903.10896
15. Á.N. Szokol, NAPLIFE Collaboration, Effect of the embedded plasmonic gold nanorods on the interaction of high intensity laser irradiation with UDMA polymer—the volume loss during crater formation, in *Talk at 11th International Conference on New Frontiers in Physics 2022, Kolymbari, Crete, Greece, 7th Sept. 2022*. https://indico.cern.ch/event/1133591/contributions/4949577/attachments/2503803/4301555/Kolymbari_2022_Agnes%20N.Szokol.pdf. Accessed 8 Dec 2024